IN-BEAM SPECTROSCOPY IN THE ACTINIDE REGION USING AN EVAPORATION RESIDUE DETECTOR*

W. Reviol, D.G. Sarantites, C.J. Chiara, M. Montero

Department of Chemistry, Washington University, St. Louis, MO 63130, USA

O.L. Pechenaya

Department of Physics, Washington University, St. Louis, MO 63130, USA

(Received November 7, 2006)

The evaporation-residue counter HERCULES, an auxiliary detector for GAMMASPHERE to perform spectroscopy in the presence of a large fission background, is described. Results from a typical experiment using the $^{26}\mathrm{Mg} + ^{198}\mathrm{Pt} \rightarrow ^{224}\mathrm{Th}^*$ reaction at 128 MeV are discussed. The discussion focuses on the new ^{220}Th level scheme. The simplex feature (alternating-parity levels) persists up to the highest spins observed. However, ^{220}Th exhibits a more vibrational-like behavior than the heavier Th isotopes. A novel interpretation for ^{220}Th based on a picture of tidal waves on a reflection-asymmetric nuclear surface is briefly reviewed. Finally, the identification of excited states in ^{219}Th is discussed.

PACS numbers: 27.60.+j, 23.20.Lv, 21.60.Cs

1. Introduction

The spectroscopy of trans-lead nuclei, *e.g.* actinide nuclei, produced in fusion-evaporation reactions is hampered by the presence of a large fission background. A "filter" or "tag" is required to separate the γ rays of the evaporation residues from those of the fission products and other sources of background. There are several, complementary approaches to meet this requirement, including the direct detection of the evaporation residues by time-of-flight (ToF) and pulse height (PH) with a dedicated detection system.

* Presented at the Zakopane Conference on Nuclear Physics, September 4–10, 2006, Zakopane, Poland.

It is desirable to choose a very asymmetric reaction, which leads, through the $\pi\lambda\!\!\!^{-2}$ factor[1], to a larger residue cross section and to less fission than in the case of a more symmetric reaction. We use the evaporation-residue counter HERCULES [1], which is optimized for experiments with GAMMASPHERE [2]. The HERCULES device is particularly suitable for very asymmetric reactions and targets with thicknesses in excess of 0.5 mg/cm^2. A benchmark experiment for the GAMMASPHERE plus HERCULES combination is the recently performed spectroscopic study of ^{220}Th [3], for which the ^{26}Mg + ^{198}Pt $\rightarrow$ ^{224}Th* ($E_{\rm lab}$ = 128 MeV) reaction was used. In this reaction, ^{220}Th+4n is the main exit channel. However, other product nuclei, including ^{219}Th + 5n, could be studied in detail as well.

After a comprehensive description of the merits of the GAMMASPHERE plus HERCULES combination, the new level scheme for ^{220}Th [3] is discussed. The original simplex-partner band (*cf.* Fig. 13 of Ref. [4]) is now observed up to $I^\pi = 22^+$ and $I^\pi = 23^-$ and a second negative-parity, odd-spin sequence has been found. An interpretation is presented supporting the picture of tidal waves on a reflection-asymmetric nuclear surface [3]. For the other nucleus of interest, ^{219}Th, a sample residue- and γ-ray gated spectrum is shown and the low-spin structure is discussed.

2. The HERCULES detector system

Prior to this work, evaporation-residue detectors have been used in several spectroscopic and reaction studies. Among those spectroscopic studies is the work done with the 18-element RFD device by Meczynski and coworkers, see *e.g.* Ref. [5].

The HERCULES device nominally consists of 64 thin fast-plastic scintillators of arc-like shape arranged in four rings. The typical angle coverage is $4.1^\circ \leq \theta \leq 25.5^\circ$ (24.1 cm target-to-detector distance). However, a part of the inner ring may be collimated to keep the individual counting rates of these detectors below 0.5 MHz. To achieve access to 25.5°, the first two rings of GAMMASPHERE are removed, *i.e.*, HERCULES is compatible with 98 GAMMASPHERE detectors in place.

The key features of HERCULES are the light-output characteristics of thin plastic scintillators for heavy ions, as discussed in Sec. 2.4 of Ref. [1], and the already mentioned high segmentation. By using the former feature, HERCULES is principally different from the RFD device. That device relies on secondary-electron detection, while HERCULES does not. The high segmentation of HERCULES helps to achieve both a high counting rate and coverage of a large fraction of the solid angle.

[1] The total fusion cross section $\sigma \propto \pi\lambda\!\!\!^{-2}\ \Sigma_\ell(2\ell+1)$ for angular momenta $\ell\hbar$.

The detection efficiency for residues is highly reaction dependent. The efficiency is determined, through the residue angular distribution, by the beam–target combination and the target thickness. A wide residue angular distribution and, thus, large HERCULES efficiency is achieved in a very asymmetric reaction (*cf.* Table I).

The GAMMASPHERE plus HERCULES setup is complementary to the setups that combine a powerful γ-ray array and a mass separator in three respects: (1) It provides an opportunity for residue-selected spectroscopy using very asymmetric reactions; beams from oxygen to silicon and targets from tantalum to lead are possible. (2) It has the capability to do detailed spectroscopy via (HI,$\alpha\, xn$) reactions. (3) It has the potential for studying short-lived isomers with a lower limit half-life ~ 65 ns; this is the sensitivity limit for *stopped* residues, given by the ToF between target and HERCULES.

TABLE I

Details of the ^{26}Mg + ^{198}Pt ($E_{\rm lab} = 128$ MeV) experiment. The ranges for certain parameter values are determined by the production of the residues at the beginning or the end of the target. Specific for this experiment is a partial collimation of the inner ring and a 0.15-mg/cm^2 Al reflector for each detector. The trigger option with HERCULES (footnote e) involves a veto for the scattered beam particles.

Beam intensity	3 pna[a] (2 pna[b])
Target thickness	0.88 mg/cm^2
$E_{\rm kin}(^{220}{\rm Th})$	4.7–11.3 MeV[c]
Flight path	24.1 cm[d]
ToF residues	65–90 ns
ToF scattered beam particles	8 ns
Angle coverage HERCULES	$\theta_{\rm min,max} = 6.1°$, 25.5°
No. HERCULES detectors	63
HERCULES efficiency	59 (4)%
No. GAMMASPHERE detectors	98
Trigger condition	GAMMASPHERE only[e]

[a]Value without the inner ring of HERCULES.
[b]Value with inner ring.
[c]Energy loss in Al leaf included.
[d]Distance between target and third ring.
[e]The condition can be also determined by HERCULES.

3. The ^{26}Mg + ^{198}Pt experiment

The ^{26}Mg $+^{198}$Pt experiment introduced above was performed at the ATLAS accelerator at Argonne National Laboratory, and the details are summarized in Table I. The γ rays from residue nuclei were selected by two-dimensional (ToF and PH) software gates. The energies of these γ rays were corrected for the Doppler shifts by using the measured residue direction. Finally, the γ-ray coincidences and angular distributions were analyzed.

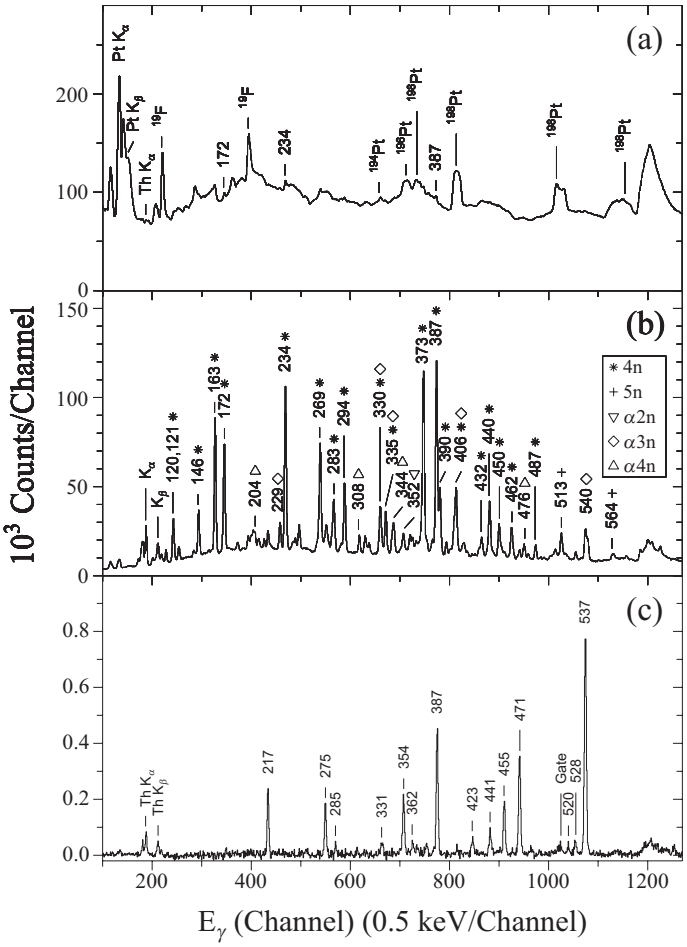

Fig. 1. Sample γ-ray energy spectra for the 128-MeV ^{26}Mg + ^{198}Pt reaction. (a) The "raw" spectrum. A fraction of the data is shown. (b) The projection of a residue-gated γ-γ coincidence matrix. Transitions are labeled by their energies in keV and symbols for the evaporation channels. The composite K X-ray peaks are also visible. (c) A residue- and γ-ray gated coincidence spectrum.

In the "raw" γ-ray spectrum of Fig. 1 (a), the peaks of interest, such as the 234-keV transition in ^{220}Th, are barely visible above background[2]. The impact of residue gating is seen in Fig. 1 (b), *i.e.*, the peak-to-background ratio has improved by two orders of magnitude. In the present reaction, the residue detection efficiency is measured to be 59(4)%. This number is based on a comparison between residue-γ–γ and "raw" γ–γ coincidence data.

The spectrum of Fig. 1 (b) shows that, in the ^{26}Mg + ^{198}Pt reaction, the xn and $\alpha\, xn$ channels compete in intensity. There is no clear evidence for the population of the 3n channel which would lead to ^{221}Th, but the spectrum contains γ rays of considerable strength that can be assigned to ^{219}Th. One of these ^{219}Th γ rays is the 513-keV line. The coincidence spectrum obtained by gating on the 513-keV γ ray is shown in Fig. 1 (c). For ^{219}Th, no excited states had been reported thus far. The isotopic assignment of prominent γ rays is based on the yield of coincident X-rays. The mass assignment to ^{219}Th is based on a technique introduced in Sec. 3.6. of Ref. [1], which is discussed hereafter.

Figure 2 shows a set of γ-ray spectra obtained by gating on different ranges of the ToF distribution of the residues. The two gates are chosen such that they enhance either the slower (a) or the faster residues (b). The gate widths are about equal. The gates change the yields of the $5n$ (crosses) and $4n$ channel (asterisks) relative to each other, as well as those of the $\alpha\, xn$ channels. Note that the quite intense 476-keV γ-ray of ^{216}Ra [6] results from a target impurity, *i.e.*, from ^{196}Pt(^{26}Mg,$\alpha 2n$). For the following argument, we consider the effect from slowing in the target. The residues that escape from the target as the slowest ones are those produced at the beginning of the target and the fastest residues are those produced at the end. Hence, the gating procedure ought to be sensitive to the slopes of the excitation functions of the $5n$ and $4n$ channels, provided that these slopes are sufficiently different.

The results from statistical model calculations with the Monte-Carlo code GEMINI [7], considering the energy range of the ^{26}Mg projectile subject to energy loss in the target, are shown in Fig. 2 (c). The ordinate values are the slopes of the calculated cross sections. In the sensitive energy range, the excitation function for ^{219}Th + $5n$ has a positive slope and is indeed maximum for $E_{\rm lab}$ at the beginning of the target (slow residues). Conversely, the $4n$ yield decreases as $E_{\rm lab}$ increases, due to a mostly negative slope. The assignment for newly observed γ rays to ^{219}Th is confirmed by an analysis of the γ-ray fold distribution. The latter quantity is obtained from the total fold of the GAMMASPHERE Ge and BGO modules with centroid values $k_\gamma = 5.5$ (^{219}Th) and 8.0 (^{220}Th).

[2] For the Doppler correction for the "raw" spectrum, the recoils are assumed to travel in the beam direction.

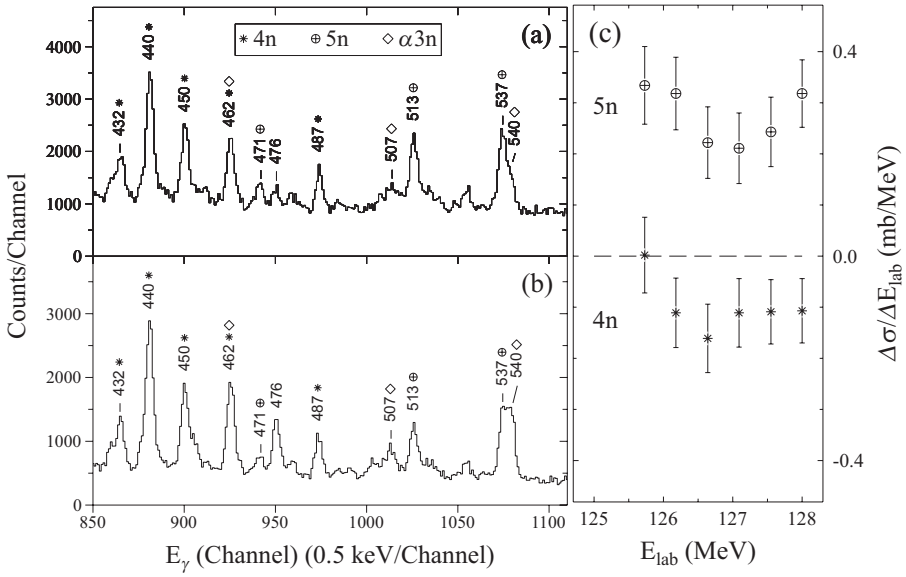

Fig. 2. Panel (a) and (b): Residue-gated total projection γ-ray spectra. The focus is on the change in yield for the ^{220}Th + 4n and ^{219}Th + 5n channels when placing different evaporation-residue ToF gates. The spectrum (a) is obtained when gating on the slower residues, the spectrum (b) when gating on the faster residues. Panel (c): Results from statistical model calculations for the dominant neutron-evaporation channels in the ^{26}Mg + ^{198}Pt reaction. The slope of the calculated cross section σ is plotted as a function of the projectile lab-energy.

4. Discussion

4.1. The level scheme of ^{220}Th

The level scheme for ^{220}Th is presented in Fig. 3. The negative-parity sequence (a), together with the positive-parity ground-state sequence, forms a simplex-partner band. There is a distinct staggering of the E1 transition energies between transitions originating from states with even and odd spins. Despite this "parity splitting", both simplex partners are present up to the highest spins observed. The B(E1)/B(E2) ratios for the simplex-partner band show a spin-dependent staggering effect (*cf.* Fig. 5 of Ref. [3]), which is in line with the above splitting.

A second negative-parity, odd-spin sequence labelled (b) is established by the 527-keV $13^-_2 \rightarrow 11^-$ E2 transition. No 19^-_2 state could be established, but a 21^-_2 state (E = 4520 keV) is observed. This state is assumed to be a member of sequence (b). The important observation is that there is a *doubling* of negative-parity, odd-spin states in ^{220}Th.

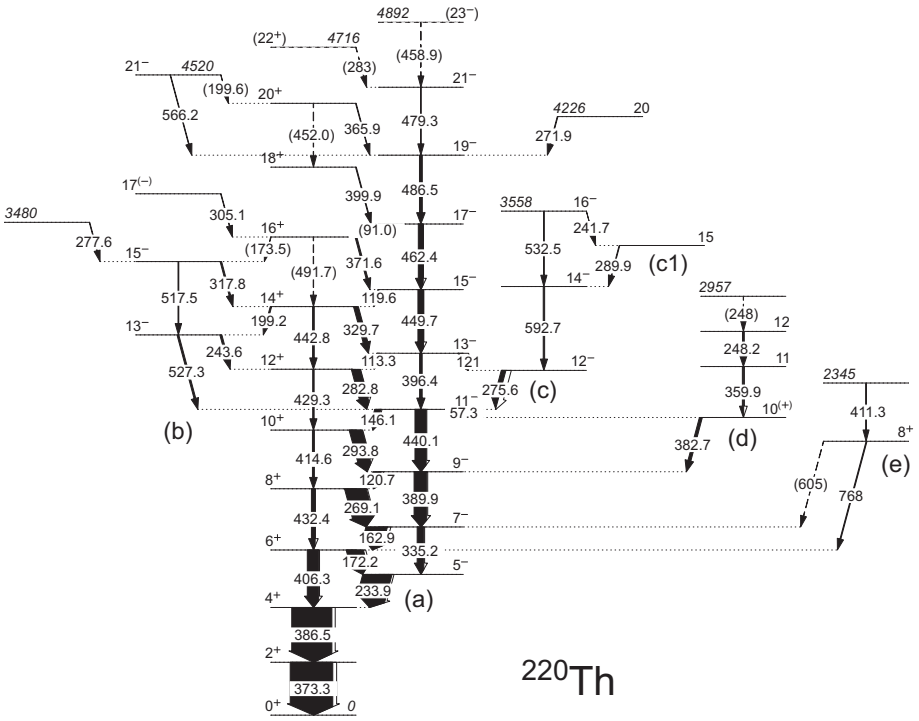

Fig. 3. The level scheme of ^{220}Th. The energy unit is keV. Transitions indicated as dashed arrows, and spins and parities given in parentheses, are considered to be tentative. Some high-lying states and the ground state are also labelled by their energy, in italics. The widths of the filled and open parts of the arrows are proportional to the γ-ray and internal-conversion intensities, respectively. The letter labels are introduced to ease the discussion.

The yrast states of ^{220}Th show the remarkable behavior of approximately constant transition energies, fluctuating around $E_\gamma \sim 420$ keV. Notably, the isotone ^{218}Ra [8] shows a very similar behavior. For the following discussion, we introduce the angular velocity $\omega \simeq E_\gamma/2\hbar$ as a useful quantity. The behavior of ^{220}Th and ^{218}Ra implies that these nuclei do not rotate faster to acquire angular momentum. Multiple band crossings taking place over a broad range of spin values I, at the same ω value in two isotones, are considered to be a highly unlikely explanation of the described behavior and an interpretation in a "traditional" nuclear rotation framework seems difficult. On the other hand, the near-equal spacing of transitions in the yrast structure cannot reflect the presence of spherical vibrational phonons either, as it extends over a large spin range. Instead, the structure of ^{220}Th seems to reflect an intermediate degree of collectivity that is currently a challenge to describe.

In Ref. [3], we proposed a new approach which considers collectivity arising from reflection-asymmetric nuclear tidal waves with a constant angular velocity, hereby retaining the simplex structure. The nuclear shape in the rotating frame of reference is a combination of quadrupole and octupole deformations which both increase with spin. The analogous $I(\omega)$ behavior was seen in "signature-partner" band structures built on K-isomers in ^{182,183}Os [9, 10], which the authors interpreted in terms of tidal waves on a triaxial nuclear surface.

The concept of tidal waves accounts also for the staggering effect. The vibrational-like motion implies tunneling between the two shapes related to each other by the operation of space inversion which restores the parity. As a consequence of the tunneling, the $B(\mathrm{E1})/B(\mathrm{E2})$ ratios exhibit a spin-dependent staggering as do the energies. The fluctuations of E_γ around an average value indicate that the realistic nuclear tidal waves have a non-adiabatic nature, in contrast to the model case of surface oscillations. When the spin of the tidal system increases, contributions by the relatively few nucleonic orbitals near the Fermi surface are still noticeable. These fluctuations can be attributed to reorientations of individual nucleonic orbitals, which, in turn, can be associated with gradual shape changes.

4.2. First observation of excited states in ^{219}Th

The ground state of ^{219}Th is presumably a $9/2^+$ state, based on a neutron $(g_{9/2})^3$ configuration, like the ground states of the lighter $N = 129$ isotones from ^{217}Ra to ^{211}Pb [6]. The spectrum of Fig. 1 (c) is representative for the sequence of E2 transitions feeding the ground state. This sequence resembles the ground-state sequence in ^{217}Ra [6]. The ^{219}Th transitions have the respective energies E_γ= 537 keV ($13/2^+ \rightarrow 9/2^+$), 513 keV ($17/2^+ \rightarrow 13/2^+$), and 471 keV ($21/2^+ \rightarrow 17/2^+$), which correspond to 540, 462, and 453 keV in the ^{217}Ra case. The lowest lying states in ^{219}Th form a vibrational-like band. This is different from the structure of ^{217}Th with an E3 ground-state transition ($t_{1/2} = 141$ ns) [11], reflecting the effect from particle–core coupling near $N = 126$. Thus, the structure of ^{219}Th indicates the gradual disappearance of single-particle-like behavior, as one departs from the singly-closed shell. A level scheme for ^{219}Th will be presented in a forthcoming publication [12].

5. Conclusions

The detection capabilities of the HERCULES device for residues from a very asymmetric fusion-evaporation reaction have been demonstrated. The reaction conditions are advantageous for two reasons: due to a rather large

$\pi\lambda\!\!\!^{-2}$ factor, the residue cross section is also rather large; and due to a wide residue angular distribution, the HERCULES detection efficiency is high. For example in the ^{26}Mg + ^{198}Pt reaction, the residue detection efficiency is 59(4)%. A typical beam intensity is 2 to 3 pnA. The coupling of HERCULES with GAMMASPHERE provides a powerful tool for detailed spectroscopy of heavy nuclei beyond lead. In the present experiment, multiple octupole-type band structures in ^{220}Th have been observed. Moreover, detailed information on excited states in ^{219}Th has been obtained for the first time. The multiphonon-like behavior of the ^{220}Th level scheme can be described, in a consistent way, by using a picture where reflection-asymmetric tidal waves travel over the nuclear surface. Nuclear tidal waves may well represent a common high-spin phenomenon in so-called transitional regions where the nuclear shape is deformation-soft.

We would like to acknowledge many important contributions to this work by the Argonne Physics Division members M.P. Carpenter, J. Greene, R.V.F. Janssens, T.L. Khoo, T. Lauritsen, C.J. Lister, J. Rohrer, D. Seweryniak, and S. Zhu. The tidal wave interpretation has been developed by S. Frauendorf (Notre Dame). The experimental setup has benefitted from assistance by J. Elson (W.U.). This work was supported by the US Department of Energy, Office of Nuclear Physics, grant no. DE-FG02-88ER-40406.

REFERENCES

[1] W. Reviol, D.G. Sarantites, R.J. Charity, C.J. Chiara, J. Elson, M. Montero, O.L. Pechenaya, S.K. Ryu, L.G. Sobotka, *Nucl. Instrum. Methods* **A541**, 478 (2005).

[2] I.Y. Lee, *Nucl. Phys.* **A520**, 641c (1990).

[3] W. Reviol *et al.*, *Phys. Rev.* **C74**, 044305 (2006).

[4] I. Ahmad, P.A. Butler, *Annu. Rev. Nucl. Part. Sci.* **43**, 71 (1993).

[5] W. Meczynski *et al.*, *Eur. Phys. J.* **A3**, 311 (1998).

[6] R.B. Firestone, V.S. Shirley, *Table of Isotopes*, 8th edition, Wiley, New York 1996.

[7] R.J. Charity, Computer code GEMINI (unpublished), `http://www.chemistry.wustl.edu/~rc.`

[8] N. Schulz *et al.*, *Phys. Rev. Lett.* **63**, 2645 (1989).

[9] L.K. Pattison *et al.*, *Phys. Rev. Lett.* **91**, 182501-1 (2003).

[10] D.M. Cullen *et al.*, *J. Phys.* **G31**, S1709 (2005).

[11] G.D. Dracoulis *et al.*, *Nucl. Phys.* **A493**, 145 (1989).

[12] W. Reviol *et al.*, to be published.